Biosilicate®–gelatine bone scaffolds by the foam replica technique: development and characterization



2013 Sci. Technol. Adv. Mater. 14 045008

(http://iopscience.iop.org/1468-6996/14/4/045008)

OPEN ACCESS
IOP PUBLISHING
SCIENCE AND TECHNOLOGY OF ADVANCED MATERIALS
Sci. Technol. Adv. Mater. **14** (2013) 045008 (11pp)
doi:10.1088/1468-6996/14/4/045008

# Biosilicate®–gelatine bone scaffolds by the foam replica technique: development and characterization

**Deborah Desimone[1], Wei Li[1], Judith A Roether[2], Dirk W Schubert[2], Murilo C Crovace[3], Ana Candida M Rodrigues[3], Edgar D Zanotto[3] and Aldo R Boccaccini[1]**

[1] Institute of Biomaterials, Department of Materials Science and Engineering, University of Erlangen-Nuremberg, Cauerstrasse 6, D-91058 Erlangen, Germany
[2] Institute of Polymer Materials, Department of Materials Science and Engineering, University of Erlangen-Nuremberg, Martensstrasse 7, D-91058 Erlangen, Germany
[3] Vitreous Materials Laboratory, Department of Materials Engineering, Federal University of São Carlos, São Carlos, São Paulo, Brazil

E-mail: aldo.boccaccini@ww.uni-erlangen.de

Received 7 April 2013
Accepted for publication 11 July 2013
Published 13 August 2013
Online at stacks.iop.org/STAM/14/045008

**Abstract**
The development of bioactive glass-ceramic materials has been a topic of great interest aiming at enhancing the mechanical strength of traditional bioactive scaffolds. In the present study, we test and demonstrate the use of Biosilicate® glass-ceramic powder to fabricate bone scaffolds by the foam replica method. Scaffolds possessing the main requirements for use in bone tissue engineering (95% porosity, 200–500 $\mu$m pore size) were successfully produced. Gelatine coating was investigated as a simple approach to increase the mechanical competence of the scaffolds. The gelatine coating did not affect the interconnectivity of the pores and did not significantly affect the bioactivity of the Biosilicate® scaffold. The gelatine coating significantly improved the compressive strength (i.e. $0.80 \pm 0.05$ MPa of coated versus $0.06 \pm 0.01$ MPa of uncoated scaffolds) of the Biosilicate® scaffold. The combination of Biosilicate® glass-ceramic and gelatine is attractive for producing novel scaffolds for bone tissue engineering.

Keywords: bioactivity, glass-ceramics, scaffolds, bone tissue engineering

## 1. Introduction

Bioactive glasses and glass-ceramics are being employed in bone tissue engineering to manufacture scaffolds to replicate bone structure, allowing the cells to adhere, proliferate, differentiate and organize into normal healthy bone as the scaffold degrades [1–5]. Besides the specific criteria for bone tissue engineering, such as osteoconductivity, biodegradability, high porosity (>90%) and pore size greater than 100 $\mu$m [6], mechanical integrity is imperative for the scaffolds to be easily manipulated by cell biologists and surgeons, and to allow their use in load-bearing implants for *in situ* bone regeneration. Hence, research has focused on the development of biodegradable scaffolds with comparable mechanical behaviour to bone [5].

Novel bioactive glass-ceramic materials are being developed in this context, considering their potential superior mechanical properties and machinability compared to the standard 45S5 Bioglass® [7, 8]. A fully crystallized glass-ceramic of the system $P_2O_5$–$Na_2O$–CaO–$SiO_2$, labelled Biosilicate®, has been developed which exhibits high bioactivity and enhanced *in vitro* bone-like tissue formation [9].



 

A recent *in vivo* study [10] showed that Biosilicate® scaffolds produced by the addition of porogen agents are biocompatible and non-cytotoxic. Moreover, since 2004, this material has been successfully tested *in vitro* and has been employed in clinical trials for the treatment of dentin hypersensitivity [11, 12].

The consolidation of glass-ceramic materials into highly porous mechanically sound scaffolds, however, is difficult by the intrinsically lower content of the residual vitreous phase, compared with (fully amorphous) glasses. On the other hand, melting of the crystalline phases present in the starting glass-ceramic material at elevated temperatures may result in the total densification of the porous structure.

This work describes the development of Biosilicate® scaffolds using the foam replica technique, originally reported for bioactive silicate systems by Chen *et al* [13]. The high interconnected porosity (>90%) obtained by the foam replica technique should lead to scaffolds that are suitable for cell invasion and vascularization during new bone formation. Reinforcement of the Biosilicate® scaffolds by gelatine coating was also investigated and the effect of the gelatine coating on the compressive strength and bioactivity of the scaffolds was assessed. The application of gelatine coatings on bioceramic scaffolds has been investigated recently, showing that such coatings can significantly improve the mechanical properties of bioactive glass and bioceramic scaffolds [14–19]. In addition, the novel gelatine-coated shell scaffolds recently developed by Bellucci *et al* [19] using a new protocol for the foam replica technique not only combine high internal porosity and an external resistant surface but also maintain the bioactivity in simulated body fluid (SBF) [19].

Previously, porous Biosilicate® scaffolds (77% open porosity and 5% closed porosity) were obtained by addition of carbon black as a porogen agent [10]. In our study, for the first time, Biosilicate® scaffolds with highly interconnected pore structure and high porosity (>90%) have been fabricated by the foam replica technique. Also for the first time, in the present investigation Biosilicate® foam-like scaffolds were surface functionalized by gelatine coating.

## 2. Experimental

### *2.1. Materials and methods*

Biosilicate® scaffolds were produced by the replica technique, according to the method described elsewhere [13]. The starting powder used consisted of a totally crystallized glass-ceramic with a particle size of 5 $\mu$m and a liquidus temperature of 1230 °C. The slurry for scaffold fabrication was prepared by dissolving polyvinyl alcohol ($M_w \sim 30\,000$, Merck, Germany) in water at a concentration of 0.01 mol $l^{-1}$ and adding the Biosilicate® powder at two investigated concentrations (40 and 60 wt.%). Polyurethane foam (45 pores per inch, Eurofoam, Germany) was employed as the sacrificial pre-form. The infiltration for 1 min was repeated two or three times, with a drying step at room temperature for 24 h between each coating.

In order to identify the most adequate temperature for scaffold sintering, the starting Biosilicate® powder was analysed in a heating microscope (Misura HSM ODHT—Expert System Solutions). The powder was manually pressed into a stainless steel mould at 25 MPa for 10 s. The sample (4 mm height × 3.2 mm diameter) was placed in an alumina plaque and inserted inside the furnace. The measurement was performed at 2 °C $min^{-1}$ up to melting. In the heating microscope, a light source is projected onto the sample and a digital camera captures the dimensional changes of its shadow [20]. The Biosilicate® powder was also analysed in a differential scanning calorimetry (DSC, NETZSCH 404) experiment using the same heating rate of 2 °C $min^{-1}$, up to 1280 °C.

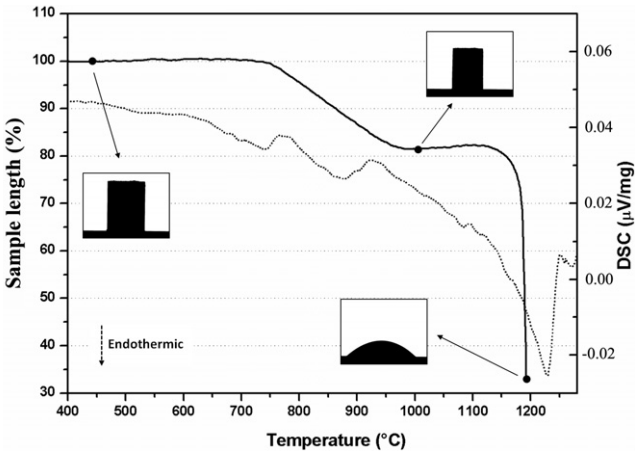


**Figure 1.** Linear shrinkage (solid line) and DSC (dashed line) curves for the Biosilicate® powder compact at a heating rate of 2 °C $min^{-1}$.


**Figure 2.** Biosilicate® scaffolds produced by the replica method using the standard slurry concentration of 40 wt.% and respective sintering temperatures employed. The scaffolds were infiltrated twice and sintered for 1 h at the selected temperatures. (Some samples were damaged during handling or were partially fractured to observe their interior region.)

Based on the linear shrinkage curve of the material, three different sintering temperatures ranging from 1050 to 1150 °C were chosen for densification of the scaffolds. For 1050 and 1100 °C, a dwell time of 1 h was selected, whereas for 1150 °C a dwell time of 30 min was chosen. A longer dwell time (2 h) was used for the thermal treatment at 1100 °C for comparison.

The scaffolds for gelatine coating were fabricated using a slurry concentration of 40 wt.%, a sintering temperature of 1100 °C and a sintering time of 2 h. Porcine skin gelatine (type A, Sigma) was used with a coating procedure similar to the method originally developed by Newby [21]. The coating solution was prepared by dissolving the gelatine in distilled water at the ratio of 5 g gelatine to 100 ml distilled


**Figure 3.** Biosilicate® scaffolds sintered at 1150 °C for 1 h, after two and three infiltration steps with slurries of 40 and 60 wt.% concentration, as indicated in the image.

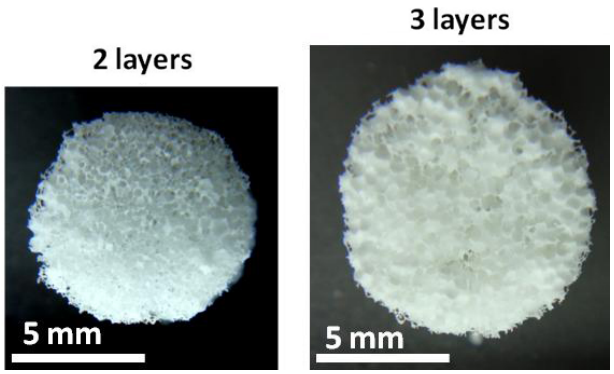


**Figure 4.** Biosilicate® scaffolds produced with a slurry concentration of 40 wt.%, with sacrificial foam infiltrated (a) two and (b) three times and sintered at 1100 °C for 2 h.

water by magnetic stirring at 60 °C. Before the dip-coating process, the scaffolds were immersed in distilled water, which was subsequently removed by compressed air before coating. Biosilicate® scaffolds with nominal dimensions of 10 mm × 5 mm × 5 mm were immersed into the gelatine–water solution for 5 min at 50 °C, while being manually shaken so that the scaffolds were coated homogeneously. After immersion, the scaffolds were dried in air at room temperature for 72 h.

### *2.2. Characterization*

Scaffolds were characterized visually using a light microscope and images were recorded by a digital camera. Microstructural characterization was carried out by scanning electron microscopy (SEM, FEI Quanta 200 FEGSEM) and x-ray diffraction (XRD, Siemens Kristalloflex D500, Bragg–Brentano, 30 kV/30 mA, Cu$K\alpha$) analysis. The density of gelatine-coated scaffolds ($\rho_{\text{scaffold}}$) was determined from the mass and volume of the scaffolds before and after coating with gelatine. The porosity before ($p_1$) and after ($p_2$) coating was calculated using the following equations:

$$p_1 = 1 - \frac{W_1}{\rho_{\text{BS}} V_1},$$

$$p_2 = 1 - \left(\frac{W_1}{\rho_{\text{BS}}} + \frac{W_2 - W_1}{\rho_{\text{gelatine}}}\right) \Big/ V_2,$$

where $W_1$ and $W_2$ are the weight of the scaffolds before and after coating with gelatine; $V_1$ and $V_2$ are the volume of the scaffolds before and after coating with gelatine; and $\rho_{\text{BS}}$ and $\rho_{\text{gelatine}}$ are the density of Biosilicate® (2.78 g cm$^{-3}$) and gelatine (1.2 g cm$^{-3}$), respectively.

The standard *in vitro* procedure described by Kokubo *et al* [22] was employed to assess the bioactivity of the scaffolds. 10 mm × 10 mm × 10 mm scaffolds were immersed in 50 ml of SBF and maintained at 37 °C in an incubator and a constant pH of 7.4. SBF was replaced twice a week during the experiments. Uncoated scaffolds were immersed in SBF for 4, 8, 24, 72 h and 1 week. The gelatine-coated scaffolds were retrieved after 1, 3, 7, 14 and 28 days of incubation. Once removed from the incubator, the samples were rinsed with deionized water and left to dry at ambient temperature in a desiccator before further examination. The presence of hydroxyapatite (HA) on the surface of the scaffolds was observed by SEM, and confirmed by Fourier transform infrared (FTIR) spectroscopy (Nicolet 6700) and XRD analyses. The SEM sample was fractured and coated by carbon. For FTIR and XRD measurements, the samples were ground and measured in powder form. FTIR spectra were collected in transmittance mode.

The compressive strength of Biosilicate® scaffolds before and after coating with gelatine was measured using a Zwick/Roell Z050 mechanical tester at a crosshead speed of 0.5 mm min$^{-1}$. The capacity of the load cell used was 50 N. The samples were rectangular in shape, with dimensions 10 mm × 5 mm × 5 mm. The compressive load was applied until 70% compressive strain was achieved in the 10 mm direction. At least five specimens were tested per sample type and the results were averaged. The work of fracture was roughly estimated as the area under the stress–strain curve up to 60% compressive strain, calculated using the software Origin®.

## 3. Results and discussion

### *3.1. Sintering of Biosilicate®*

The linear shrinkage curves of the Biosilicate® powder obtained by heating microscopy and DSC results are shown in figure 1. The heating microscopy and DSC experiments were performed at a heating rate of 2 °C min$^{-1}$, as used for

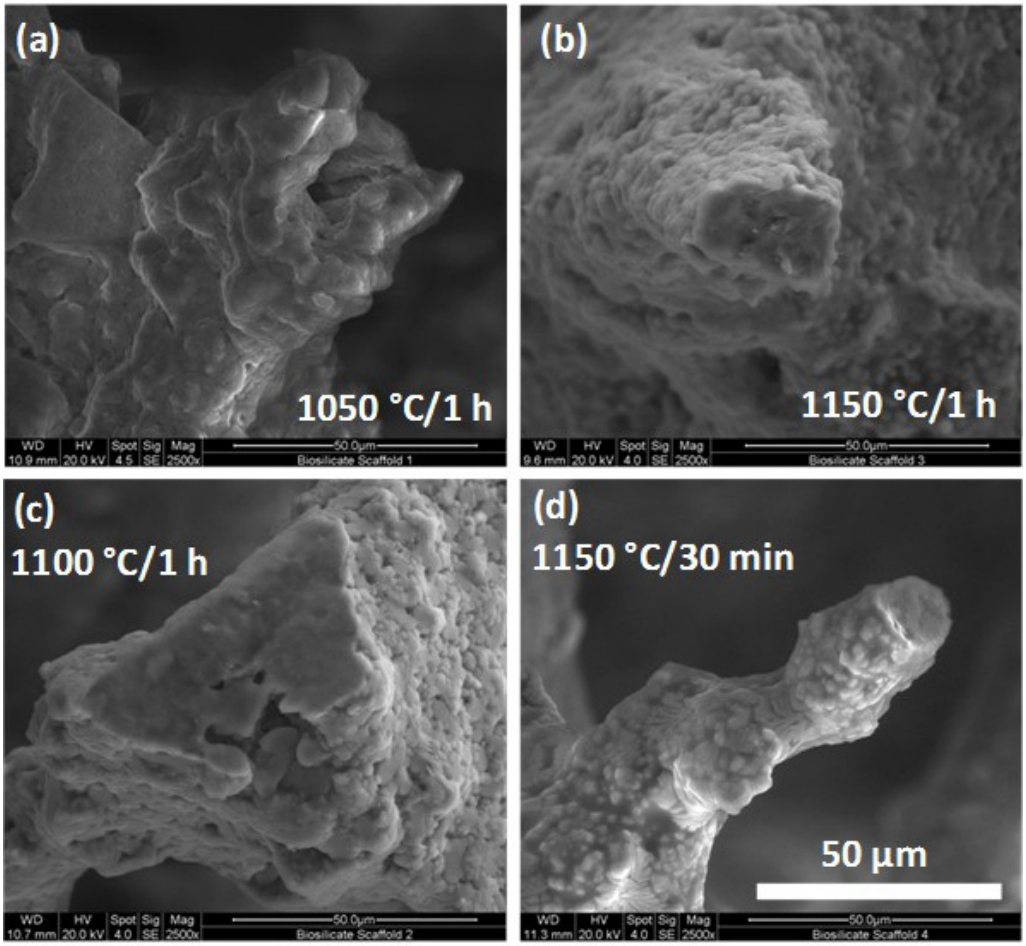


**Figure 5.** SEM images of fracture surfaces of Biosilicate® scaffolds showing strut densification after sintering at increasing temperatures (a)–(c), as well as after reducing the holding time at the highest sintering temperature (d).

manufacturing scaffolds by the replica technique. The curve shows the onset of sintering at approximately 750 °C. The beginning of the sintering process coincides with the first endothermic peak in the DSC curve (dashed line—figure 1). Linear shrinkage of the powder compact continues until saturation occurs at 975 °C, when shrinkage reaches a value of 18% and a second endothermic peak is observed in the DSC curve. At 1075 °C, a small expansion (∼1%) probably related to a degassing phenomenon occurs. Complete softening of the sample is observed above 1120 °C, before the third endothermic peak.

Above 1000 °C, after sufficient liquid formation, sintering should occur rapidly and effectively by viscous flow. To obtain mechanically competent scaffolds, full densification of the struts is required. Based on these results, three temperatures were initially selected for investigating their suitability for scaffold manufacturing: 1050, 1100 and 1150 °C.

### *3.2. Optimization of scaffold production*

Biosilicate® scaffolds produced by the replica method using a 40 wt.% slurry infiltrated twice into the sacrificial foam and sintered at 1050, 1100 and 1150 °C for 1 h are shown in figure 2. The scaffolds produced under the three different temperatures were all qualitatively and macroscopically sound (e.g. mechanically stable), although those sintered at 1050 °C were relatively more fragile than those produced at 1150 °C, which were apparently the strongest (when initially assessed by manual handling).

Further sintering treatments were thus performed at 1150 °C for 1 h, in this case assessing the use of a slurry with higher Biosilicate® powder concentration (60 wt.%) and repeating the infiltration three times (figure 3).

The scaffolds produced with the slurry of higher glass-ceramic powder concentration exhibited a structure with closed porosity and apparently higher deformation, attributed to the higher content of liquid phase during sintering. Light microscope images showed that even the scaffolds produced with the 40 wt.% slurry exhibited some closed pores, indicating that the temperature of 1150 °C was excessively high. Sintering at 1100 °C for 2 h, on the other hand, resulted in scaffolds with an open pore structure and good mechanical integrity (e.g. qualitatively assessed by manual handling), similar to those sintered at 1150 °C. Typical images of these scaffolds are shown in figure 4.

Sintering for 2 h at 1050 °C was also performed, as well as for 30 min at 1150 °C. The former did not improve strength significantly (as assessed by manual handling), while the latter

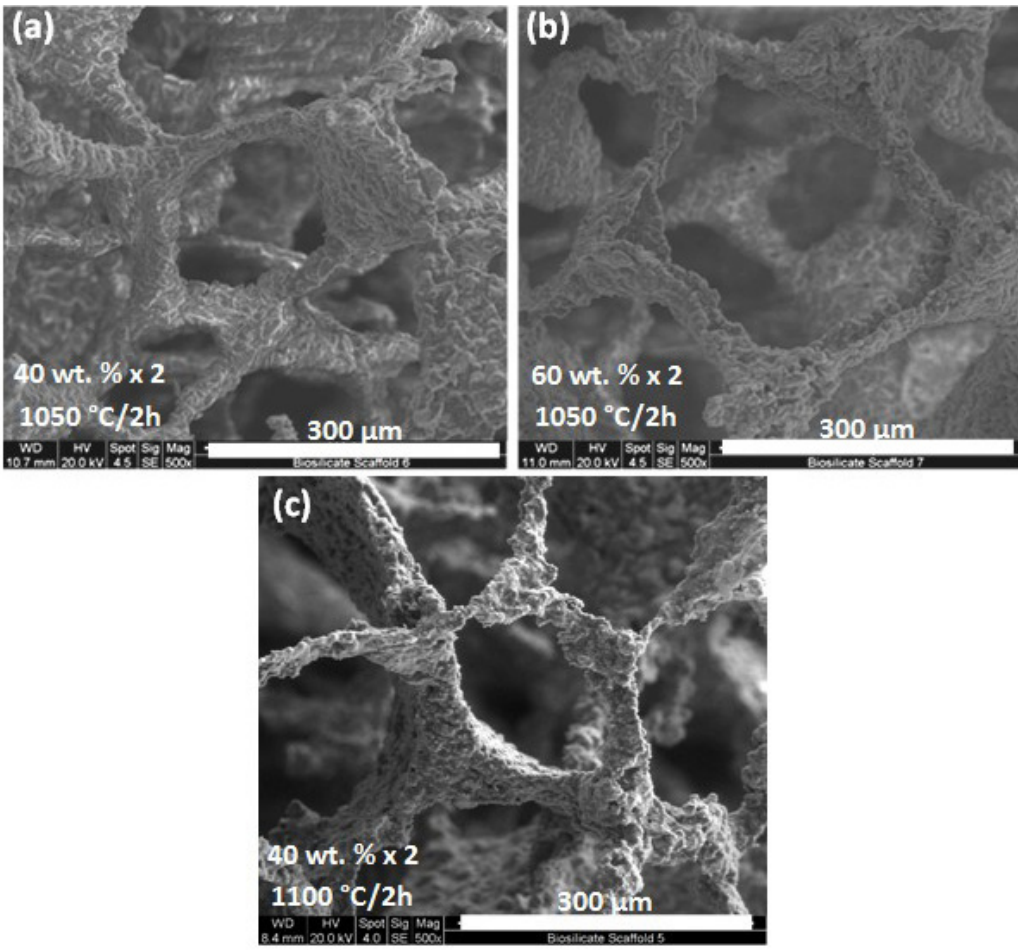


**Figure 6.** SEM images of Biosilicate® scaffolds produced from 40 wt.% ((a) and (c)) and 60 wt.% (b) slurries and sintered at 1050 and 1100 °C for 2 h, showing strut microstructure and larger pores obtained from the slurry of higher concentration.

resulted in sound scaffolds, but did not improve deformation and pore closure. In this preliminary assessment of scaffold integrity, manual handling to determine the scaffold's stability was considered a suitable qualitative method as scaffolds that were fractured during handling were discarded for further studies.

Increasing the sintering temperature resulted in the densification of struts, as expected (figures 5(a)–(c)), due to increased vitrification at temperatures above 1050 °C, even using a shorter holding time at the highest temperature employed (1150 °C) (figure 5(d)). This result explains the qualitatively higher mechanical resistance observed for the samples sintered at temperature above 1100 °C, as the mechanical strength of scaffolds is strongly dependent on the microstructure homogeneity and density of the individual struts.

Scaffolds produced with the slurry of higher concentration (60 wt.%) exhibited larger pores, as a result of the higher densification upon sintering (figures 6(a) and (b)). In all cases the pore sizes were greater than 100 $\mu$m, as generally required for use in tissue engineering [5, 6]. Scaffolds sintered at 1100 °C for 2 h exhibited similar microstructure to those sintered at 1050 °C for 2 h (figure 6(c)), and were qualitatively more resistant.

Figure 7 shows strut densification in scaffolds sintered at 1100 °C, which explains the higher mechanical resistance of these scaffolds.

XRD analyses (figure 8) revealed a crystalline structure consisting of a mixture of silicate and phosphate phases similar to those in powder diffraction files 01-075-1687 and 01-081-2266, as well as alumina (the minor alumina phase detected is likely due to the alumina substrate used to sinter the scaffolds). These results confirmed that thermal processing at up to 1150 °C did not alter the crystalline structure of the material.

Overall, scaffolds manufactured using the 40 wt.% concentrated slurry and thermal-treated at 1100 °C for 2 h resulted in an optimal combination of porosity, morphology, mechanical resistance (qualitatively assessed) and strut microstructure. This was therefore selected as the optimal processing route for the production of Biosilicate® scaffolds described in the following sections.

### *3.3. Gelatine-coated scaffolds*

The typical microstructure of scaffolds before and after coating with gelatine is shown in figure 9, where a highly interconnected structure is observed. The pore sizes were

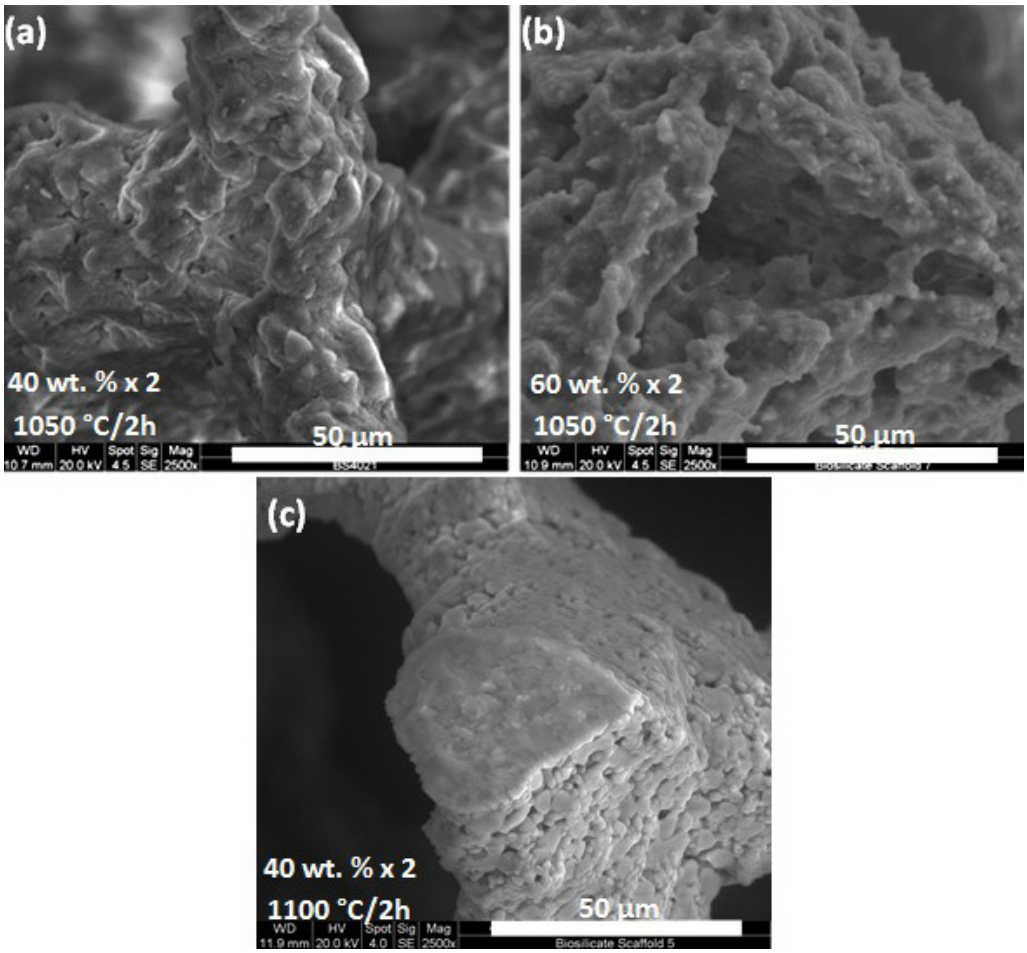


**Figure 7.** SEM images of fracture surfaces of scaffolds showing open ((a) and (b)) and densified struts in Biosilicate® scaffolds fabricated from the indicated slurry concentrations and sintered at 1050 and 1100 °C, respectively, for 2 h.

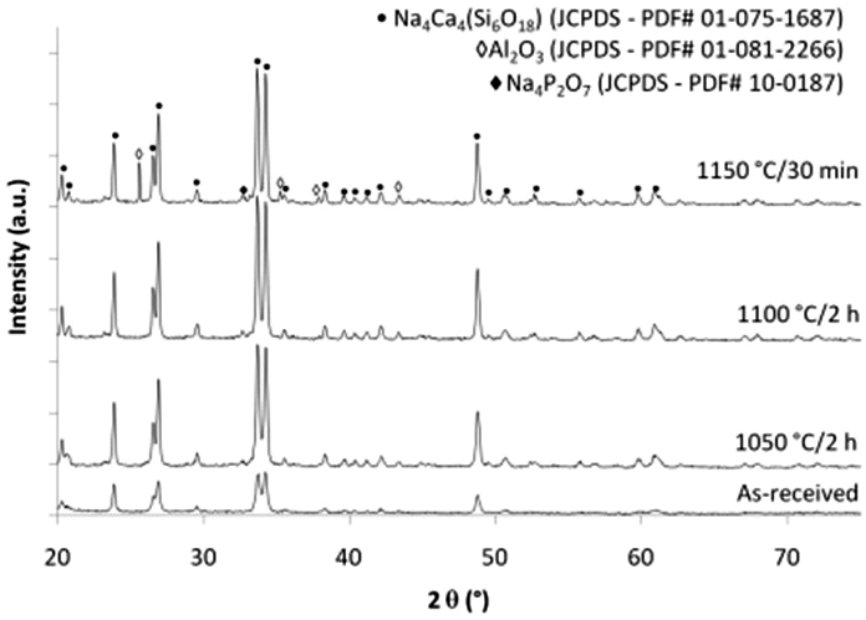


**Figure 8.** XRD patterns of Biosilicate® powder before and after sintering at increasing temperatures. The crystalline structure of the material is not altered by the thermal process.

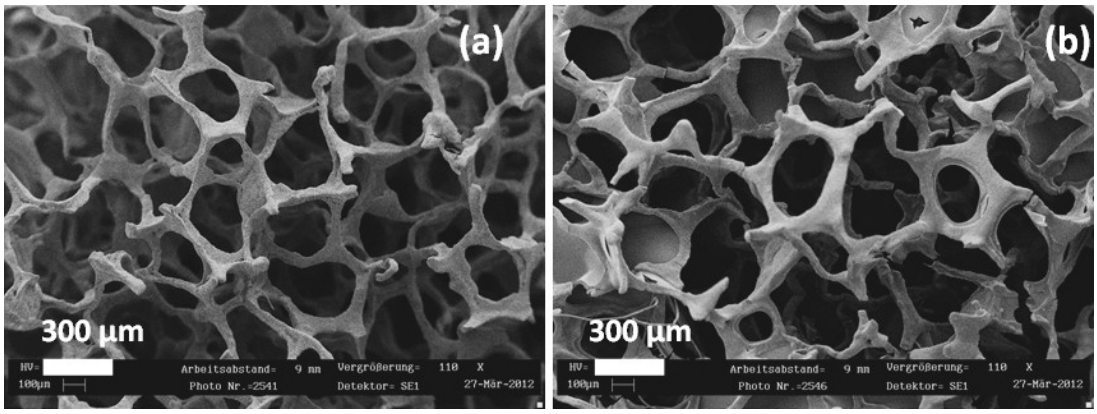


**Figure 9.** Biosilicate® scaffolds (a) before and (b) after coating with gelatine.

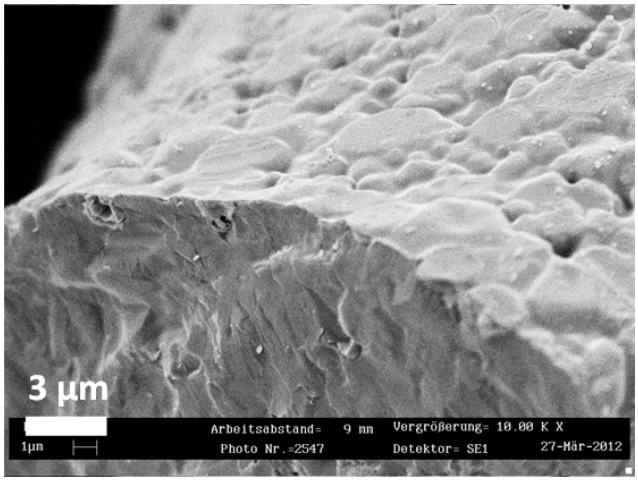


**Figure 10.** Surface morphology of a Biosilicate® scaffold strut coated by gelatine.

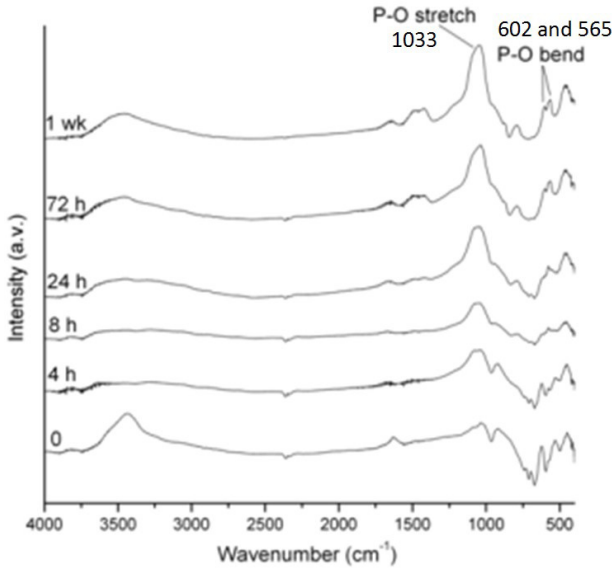


**Figure 11.** FTIR absorption spectra of uncoated Biosilicate® scaffolds before (zero) and after immersion in SBF for increasing times up to one week.

measured from SEM images to be in the range of 200–500 $\mu$m (average size of 350 $\mu$m), which is in the desired range for application in bone tissue engineering [5, 6]. The calculated porosity values of scaffolds before and after gelatine coating were 95 and 93%, respectively, i.e. a reduction of only 2% was observed after gelatine coating. The gelatine content in the scaffolds was on average 15.3 wt.%. The open pore structure of sintered scaffolds was retained after coating with gelatine, with only a few of the pores being blocked by the coating (figure 9(b)).

The typical surface morphology of a strut of a coated scaffold is shown in figure 10, indicating that the strut surface was covered by gelatine and most of the micropores on the strut were infiltrated by the polymer. The gelatine coating is not homogeneous due to the roughness of the original struts. Moreover some micropores were not infiltrated by the polymer, providing channels for SBF to be in direct contact with the bioactive material underneath the coating.

### *3.4. Bioactivity investigation*

The *in vitro* bioactivity test in SBF indicated the formation of crystalline hydroxycarbonate apatite (HCA) on uncoated sample surfaces after immersion for over 72 h, as indicated in the FTIR spectra (figure 11). The vibrational bands at 565 and 602 $cm^{-1}$ corresponding to the P–O bending vibrations of $PO_4^3$-tetrahedra in crystalline HCA were present in the respective spectra (72 h and 1 week). These characteristic vibrational bands were not observed in the spectra of samples immersed for shorter times (e.g. 24, 8 and 4 h).

SEM images of uncoated scaffolds after immersion in SBF confirmed the formation of HCA, as shown in figure 12. The characteristic HCA features are observed on samples after 72 h, while the $SiO_2$-gel layer which usually forms at the initial ion-exchange stages prior to HCA formation was observed in the images of samples immersed for 4–24 h. The amount of HCA is qualitatively confirmed to increase with increasing immersion time in SBF. The image of the sample immersed in SBF for 3 weeks shows a fractured area, exposing the unreacted material in the core of a strut covered by HCA, where the thickness of the HCA layer can be estimated to be approximately 1 $\mu$m (figure 12).

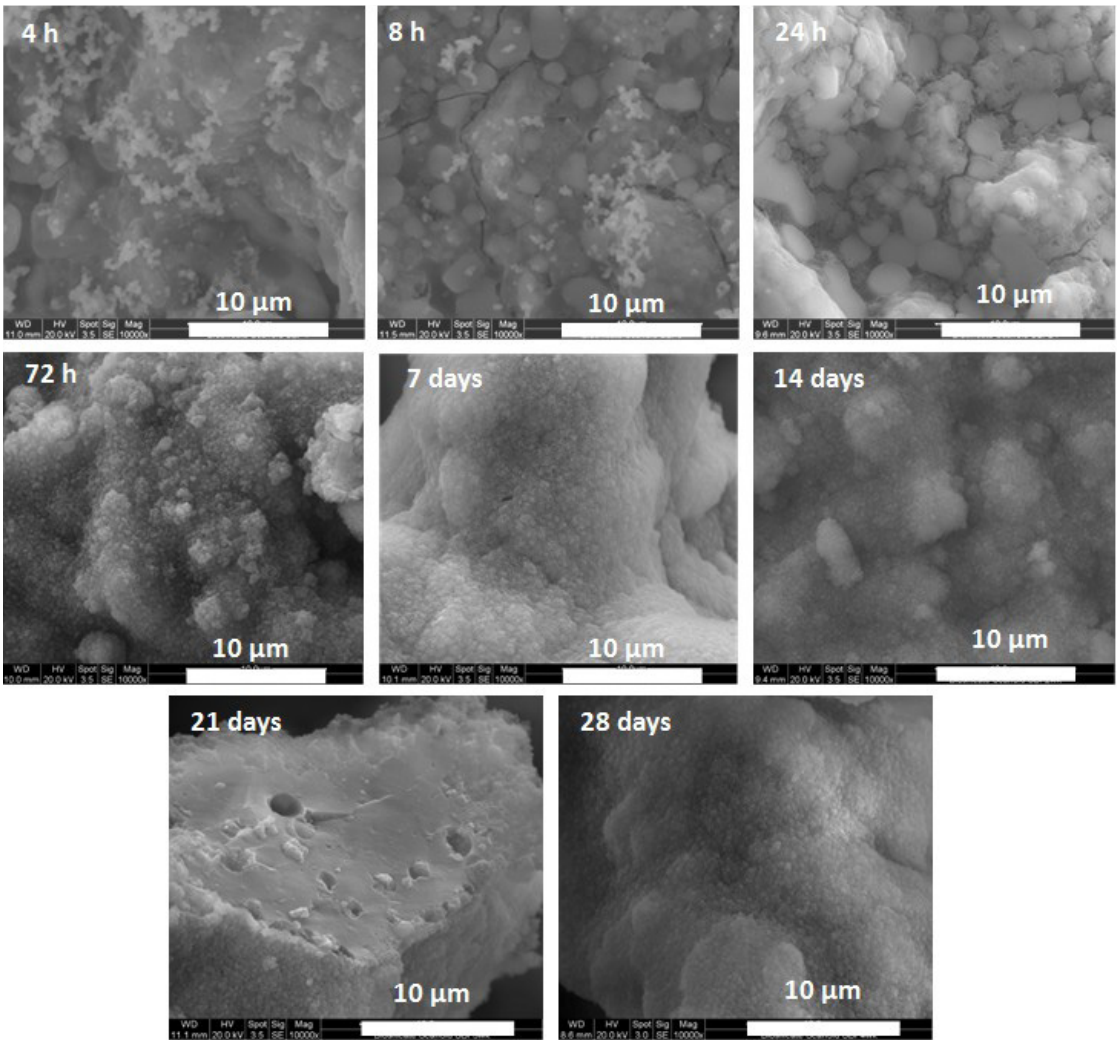


**Figure 12.** SEM images of uncoated Biosilicate® scaffolds after immersion in SBF for the indicated time periods showing progressive formation of an HCA layer with increasing immersion time in SBF.

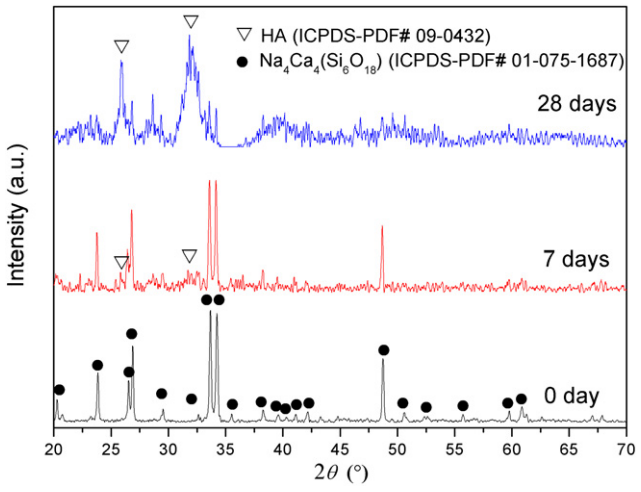


**Figure 13.** XRD spectra of gelatine-coated scaffolds before and after immersion in SBF for 7 and 28 days. The major peaks of $Na_4Ca_4(Si_6O_{18})$ and the HA phase are marked by (●) and (▽), respectively.

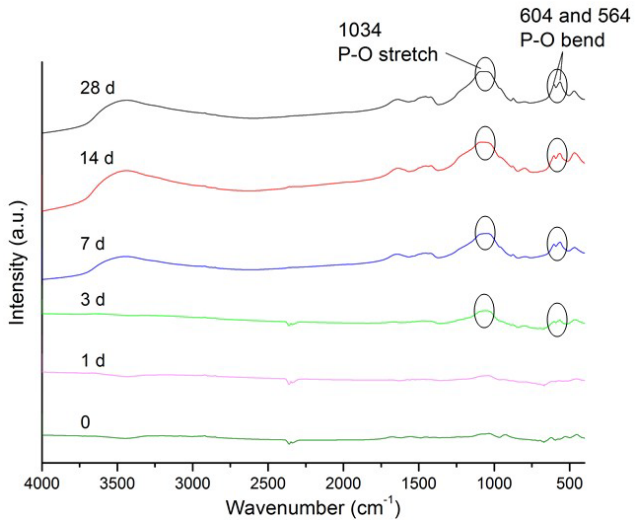


**Figure 14.** FTIR absorption spectra of gelatine-coated scaffolds before and after immersion in SBF for 1, 3, 7, 14 and 28 days.

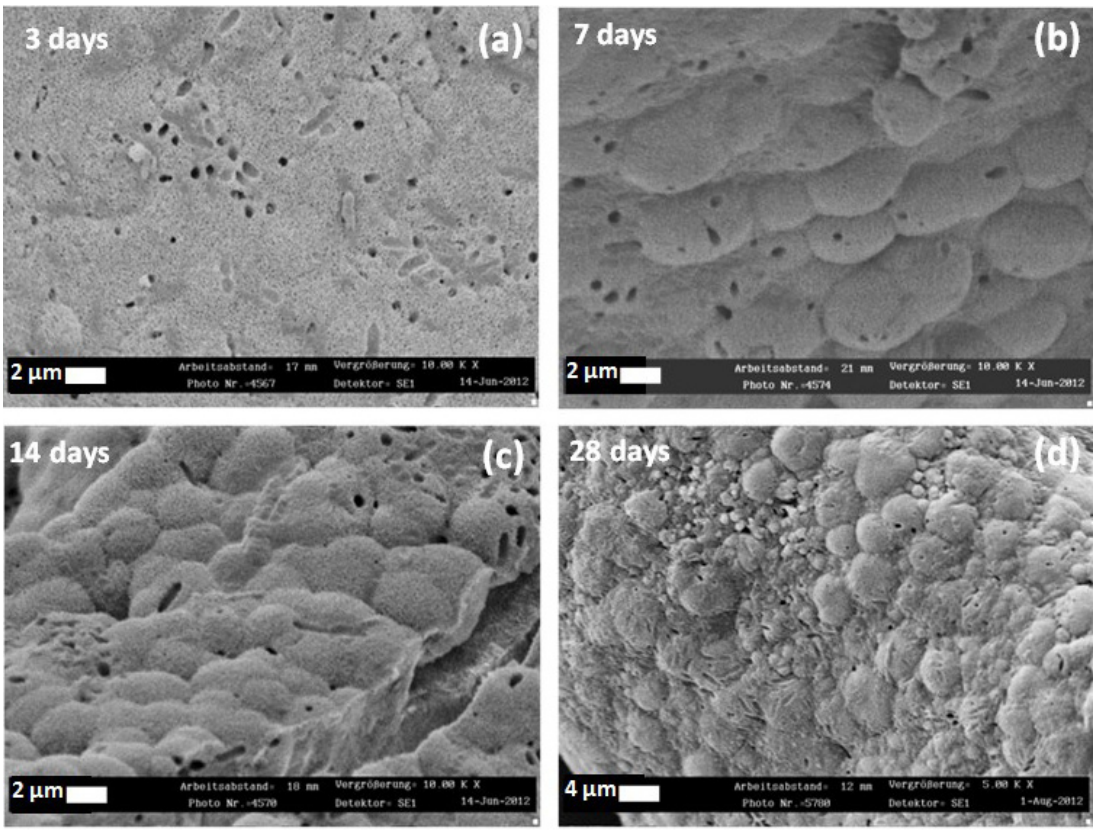


**Figure 15.** SEM micrographs showing HA formation on the surfaces of gelatine-coated scaffolds after immersion in SBF for (a) 3, (b) 7, (c) 14 and (d) 28 days.

Figure 13 shows the XRD spectra of coated scaffolds before and after immersion in SBF for up to 4 weeks. Before immersion in SBF, the crystalline phase was identified as the characteristic sodium–calcium–silicate structure $Na_4Ca_4(Si_6O_{18})$ (see also figure 8). HA peaks were observed on coated scaffolds after immersion in SBF for 7 days, indicating that the material's bioactivity was not significantly compromised by the presence of the gelatine coating.

Figure 14 presents the FTIR spectra of coated scaffolds before and after immersion in SBF for 1, 3, 7, 14 and 28 days. After 3 days of immersion, two small peaks were observed at ∼564 and ∼604 $cm^{-1}$ and a slight shift of the peak at ∼1034 $cm^{-1}$, which can be attributed to the deposition process of calcium and phosphate groups. The characteristic peaks of HA became sharper as the immersion time in SBF increased, indicating the increase in crystallinity. Thus FTIR characterization confirmed that both uncoated and coated scaffolds exhibited rapid formation of HA, and that, qualitatively considered, the gelatine coating did not significantly reduce the bioactivity of Biosilicate® scaffolds.

As shown in figure 15, the formation of HA-like crystalline apatite on the surface of gelatine-coated scaffolds after immersion in SBF for 3 days was confirmed by SEM observation. HA crystals can be recognized as the globular, cauliflower-shaped structures on the scaffold's surface. After 3 days, the HA layer formed was not homogeneous (figure 15(a)). However, after 7 days, the HA layer was seen to have grown and exhibits homogeneous morphology (figures 15(b)–(d)). Thus, it is confirmed that HA crystals grow on the surface of the scaffold, and the presence of the coating (which is not a continuous layer as discussed above) did not significantly hinder the formation of HA. Even if XRD, FTIR and XRD results do not seem to indicate a negative effect of the gelatine coating on bioactivity, it is likely that the start of HA growth occurs earlier in the uncoated scaffolds (e.g. compare figures 11 and 15). In order to confirm this suggestion, a more detailed analysis at the initial period of immersion (<1 day) should be carried out.

### *3.5. Mechanical properties*

Typical compressive stress–strain curves of uncoated and coated scaffolds are shown in figure 16. The average compressive strength of non-coated and coated scaffolds was determined to be $0.06 \pm 0.01$ and $0.80 \pm 0.05$ MPa, respectively. The area under the stress–strain curve of the gelatine-coated scaffold, which represents an indication of the work of fracture, was calculated to be 77.6 N mm, compared to 2.55 N mm for the non-coated scaffolds, demonstrating the improvement in the material's toughness under compression. In addition, the gelatine-coated scaffolds did not collapse after the compressive strength test, while the non-coated scaffolds were crushed to powder.

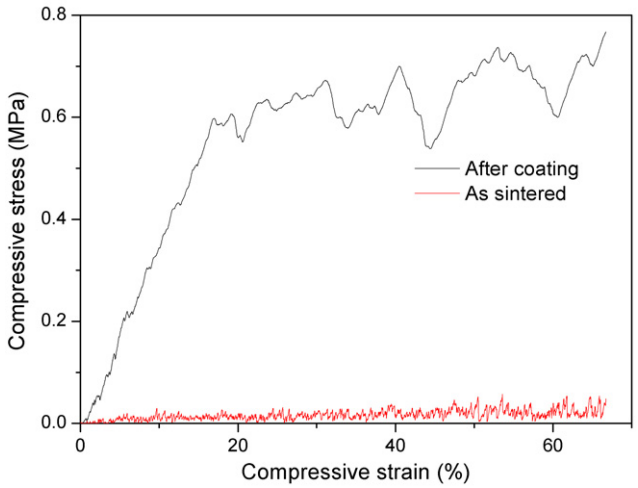


**Figure 16.** Typical compressive stress–strain curves of the as-sintered scaffold and the gelatine-coated scaffold.

Moreover, despite only reducing porosity by ∼2%, the gelatine coating infiltrated the micropores and microcracks in the struts, improving the mechanical stability of the flaw sensitive material and making the originally weak and brittle struts stronger and tougher. Similar results have been obtained in the previous study combining gelatine as a coating on Bioglass®-based scaffolds [14] and by Liu *et al* [15] in a study on gelatine-coated porous HA/tricalcium phosphate bioceramics. The micron-scale crack-bridging mechanism, previously investigated by Pezzotti and Asmus [23], was proposed to explain strengthening and toughening in this type of polymer-ceramic composite, which is evident by the presence of polymer ligaments that were stretched along the crack wake upon crack opening. Indeed polymer coating of highly porous and brittle scaffolds is an attractive approach being increasingly considered to fabricate tough and mechanically sound scaffolds [7, 14, 24–28].

It is generally accepted that the compressive strength of cancellous bone is in the range of 0.2–4 MPa when the relative density is about 0.1 [29]. Although the measured compressive strength of the present scaffolds (0.80 MPa) falls closer to the lower limit of this range, it is sufficient for the scaffolds to be handled safely by cell biologists and surgeons, due to the toughening effect of the gelatine coating, making the composite material a promising candidate for application in bone tissue engineering.

## 4. Conclusions

Scaffolds possessing the necessary requirements for use in bone tissue engineering (95% porosity, 200–500 $\mu$m pore size) were produced from a fully crystalline silicate (Biosilicate®) powder. The material exhibited good sinterability at temperatures around the vitrification temperature of the Biosilicate® composition, without modifying its crystalline structure. *In vitro* bioactivity assessment in SBF indicated that the material's intrinsic bioactivity was not affected by the thermal processing. The mechanical integrity of the scaffolds was increased by coating the scaffolds with a thin gelatine layer. The gelatine coating did not affect pore interconnectivity of the scaffolds and the scaffold's bioactivity was not significantly reduced by the gelatine coating. Significant improvements in compressive strength and the work of fracture were achieved by the presence of the gelatine coating. Future efforts will concentrate on *in vitro* and *in vivo* studies of the composite gelatine–Biosilicate® scaffolds, as a novel system with potential for application in bone tissue engineering.

## Acknowledgments

WL acknowledges the China Scholarship Council (no. 2011628002) for financial support. The Brazilian authors are grateful to FAPESP (grant number 2013/07793-6), CNPq and Capes for their generous funding and University of Erlangen-Nürnberg within the funding program 'Open Access Publishing' (http://www.ub.uni-erlangen.de/open-access/).

## References

[1] Baino F and Vitale-Brovarone C 2011 *J. Biomed. Mater. Res.* A **97A** 514
[2] Rahaman M N, Day D E, Bal B S, Fu Q, Jung S B, Bonewald L F and Tomsia A P 2011 *Acta Biomater.* **7** 2355
[3] Bellucci D, Chiellini F, Ciardelli G, Gazzarri M, Gentile P, Sola A and Cannillo V 2012 *J. Mater. Sci. Mater. Med.* **23** 1397
[4] Jones J R and Hench L L 2003 *J. Mater. Sci.* **38** 3783
[5] Gerhardt L C and Boccaccini A R 2010 *Materials* **3** 3867
[6] Guarino V, Causa F and Ambrosio L 2007 *Expert Rev. Med. Dev.* **4** 405
[7] Wu C, Ramaswamy Y, Boughton P and Zreiqat H 2008 *Acta Biomater.* **4** 343
[8] Baino F, Ferraris M, Bretcanu O, Verne E and Vitale-Brovarone C 2013 *J. Biomater. Appl.* **27** 872
[9] Moura J, Teixeira L N, Ravagnani C, Peitl O, Zanotto E D, Beloti M M, Panzeri H, Rosa A L and de Oliveira P T 2007 *J. Biomed. Mater. Res.* A **82A** 545
[10] Kido H W, Oliveira P, Parizotto N A, Crovace M C, Zanotto E D, Peitl-Filho O, Fernandes K P S, Mesquita-Ferrari R A, Ribeiro D A and Renno A C M 2013 *J. Biomed. Mater. Res.* A **101A** 667
[11] Tirapelli C, Panzeri H, Soares R G, Peitl O and Zanotto E D 2010 *Braz. Oral Res.* **24** 381
[12] Tirapelli C, Panzeri H, Lara E H G, Soares R G, Peitl O and Zanotto E D 2011 *J. Oral Rehab.* **38** 253
[13] Chen Q Z, Thompson I D and Boccaccini A R 2006 *Biomaterials* **27** 2414
[14] Metze A L, Grimm A, Nooeaid P, Roether J A, Hum J, Newby P J, Schubert D W and Boccaccini A R 2013 *Key Eng. Mater.* **541** 31
[15] Liu B, Lin P, Shen Y and Dong Y 2008 *J. Mater. Sci. Mater. Med.* **19** 1203
[16] Dressler M, Dombrowski F, Simon U, Börnstein J, Hodoroaba V D, Feigl M, Grunow S, Gildenhaar R and Neumann M 2011 *J. Eur. Ceram. Soc.* **31** 523
[17] Erol M, Ozyuguran A, Ozarpat O and Kucukbayrak S 2012 *J. Eur. Ceram. Soc.* **32** 2747
[18] Komlev V S, Barinov S M and Rustichelli F 2003 *J. Mater. Sci. Lett.* **22** 1215
[19] Bellucci D, Sola A, Gentile P, Ciardelli G and Cannillo V 2012 *J. Biomed. Mater. Res.* A **100A** 3259

[20] Boccaccini A R, Stumpfe W, Taplin D M R and Ponton C B 1996 *Mater. Sci. Eng.* A *Struct. Mater.* **219** 26
[21] Newby P 2013 *PhD Thesis* Department of Materials Imperial College, London
[22] Kokubo T, Ito S, Huang Z, Hayashi T, Sakka S, Kitsugi T and Yamamuro T 1990 *J. Biomed. Mater. Res.* **24** 331
[23] Pezzotti G and Asmus S M F 2001 *Mater. Sci. Eng.* A *Struct. Mater.* **316** 231
[24] Yunos D M, Bretcanu O and Boccaccini A R 2008 *J. Mater. Sci.* **43** 4433
[25] Peroglio M, Gremillard L, Chevalier J, Chazeau L, Gauthier C and Hamaide T 2007 *J. Eur. Ceram. Soc.* **27** 2679
[26] Kim H W, Knowles J C and Kim H E 2004 *Biomaterials* **25** 1279
[27] Nie L, Chen D, Yang Q, Zou P, Feng S, Hu H and Suo J 2013 *Mater. Lett.* **92** 25
[28] Yang G, Yang X, Zhang L, Lin M, Sun X, Chen X and Gou Z 2012 *Mater. Lett.* **75** 80
[29] Gibson L J and Ashby M F 1999 *Cellular Solids: Structure and Properties* (Cambridge: Cambridge University Press)